

Chemical Composition and Evolution of Irregular and Blue Compact Galaxies

J. Lequeux*, M. Peimbert**, J. F. Rayo, A. Serrano, and S. Torres-Peimbert**

Instituto de Astronomía, Universidad Nacional Autónoma de México, Apdo. Postal 70-264, México 20, D. F. México

Received December 27, 1978

Summary. We present new spectrophotometric observations of H II regions in the irregular galaxies NGC 4449, NGC 6822, and IC 10 and in the blue compact galaxies I Zw 18, II Zw 40, and II Zw 70. These observations are used to derive abundances of He, N, O, Ne, S, and Ar relative to H. By extrapolation of the He/H vs O/H relation a pregalactic value of $N(\text{He})/N(\text{H}) = 0.074 \pm 0.006$ is found. Our results are consistent with the solution that nitrogen is in part a product of primary nucleosynthesis and that the ratio of primary production of nitrogen to oxygen is $N/\text{O} \approx 2 \cdot 10^{-2}$. Over the mass range covered by our sample of galaxies (about two orders of magnitude) it is found that: a) the heavy element yield is constant and given by $p = 0.004 \pm 0.001$, b) the heavy element abundance and the total mass of the galaxies are related by $\log M_T = (8.5 \pm 0.4) + (190 \pm 60)Z$. Excellent agreement is obtained between a model of galactic chemical evolution and the observations; the model is based on a new initial mass function and on stellar evolutionary models with mass loss by Chiosi and collaborators. We find that irregular and blue compact galaxies seem to differ only in the present rate of star formation; however we are still unable to decide whether they are old systems with a present burst, or systems where star formation has started only recently, although the former hypothesis is somewhat favored.

Key words: compact galaxies – irregular galaxies – interstellar abundances – galactic evolution – H II regions

I. Introduction

The determination of element abundances in irregular and blue compact galaxies is of particular interest because these systems are relatively unevolved. Their large hydrogen mass to total mass ratios (Fisher and Tully, 1975; Chamaraux, 1977) as well as their large underabundances in heavy elements (see e.g. Searle and Sargent, 1972; Peimbert and Torres-Peimbert, 1974, 1976; Peimbert, 1975) show that a relatively small fraction of their gas has been processed into stars. Moreover, their low total mass makes

Send offprint requests to: J. Lequeux

* On leave from the Observatoire de Meudon, F-92190 Meudon, France

** Visiting Astronomer, Kitt Peak National Observatory, which is operated by the Association of Universities for Research in Astronomy, Inc., under contract with the National Science Foundation.

accretion of any extragalactic material very inefficient (Hunt, 1971), contrary to what may happen in more massive spiral galaxies. Their relative lack of evolution, their simple structure with respect to that of spiral galaxies, and their isolated nature, make them choice objects for studying galactic evolution.

These galaxies are particularly useful for the study of the early evolution of the chemical composition. It is known (Talbot and Arnett, 1973) that the instant recycling approximation is valid for the study of the enrichment of the interstellar medium due to massive stars, so that the present abundances of primary elements, like ^{16}O , are independent of the detailed history of the galaxy and depend only on: a) the total amount of matter processed into stars, b) the Initial Mass Function, IMF, and c) the nucleosynthetic properties of stars (for a general review of chemical evolution of galaxies see Audouze and Tinsley, 1976). In particular, all primary elements produced by massive stars should behave similarly since their depletion by conversion into secondary elements is not very important.

We shall use the new observations of unevolved systems reported here, together with other observations, to derive: a) the primeval abundance of helium, by extrapolating the (He/H) vs (O/H) relation to zero oxygen abundance, b) a tentative estimate of the fraction of ^{14}N produced by primary processes, by studying the (N/O) vs (O/H) relation, c) the heavy element content versus the total galactic mass relation, d) the heavy element yield, $p(Z)$, by means of the (O/H) versus $(M_{\text{gas}}/M_{\text{tot}})$ relation; e) finally these results will be compared with galactic evolution models to try to put limits on the evolutionary properties of irregular and blue compact galaxies.

In Sect. II the new observations are described. In Sect. III the abundances of the elements are derived. In Sect. IV the gaseous and total masses of the considered galaxies are presented. In Sect. V the models of chemical evolution are described. In Sect. VI the models are compared with the observations, and the conclusions are summarized in Sect. VII.

II. Observations

We decided to study the blue compact galaxies I Zw 18 = Markarian 116, II Zw 40, and II Zw 70 as well as some of the brightest H II regions in irregular galaxies: in NGC 4449, region 39 of Crillon and Monnet (1969); in NGC 6822, regions V and X of Hubble (1925); and in IC 10, regions 1 and 2 defined in Fig. 1.

The observations were carried out in 1977–1978 at KPNO with the 2.1 m telescope and the Image Intensifier Dissector Scanner, IIDS. The IIDS is a dual beam multichannel spectrom-

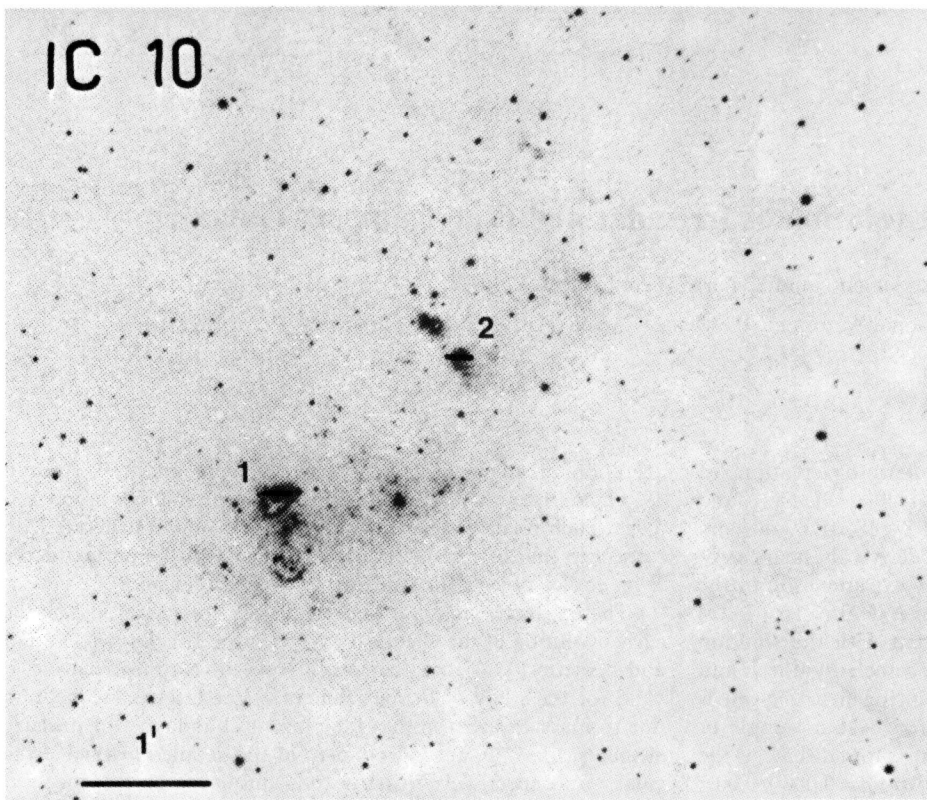


Fig. 1. H α plate of IC 10 by Sandage and Tammann (1974). In this picture we identify the observed regions 1 and 2

eter that was used with the Gold image tube spectrograph and the Wynne camera. It has a cooled RCA glass, 3-stage magnetically focused image tube with a S-20 photocathode and a P-11 phosphor. The two spectra are scanned by an ITT image dissector tube whose scanning aperture is $50 \mu \times 250 \mu$ in size, where the first number is along and the second perpendicular to the dispersion. Each spectrum of about 21 mm is recorded into 1024 channels. The dual entrance slits used were 0.30×0.98 mm where the first value is along, and the second perpendicular, to the dispersion; they correspond to $3''.8 \times 12''.4$ on the plane of the sky. In all cases reported here the slits were oriented east west, the separation between the centers of both slits corresponds to $99''$. Two gratings, at a dispersion of 86 \AA/mm , were used to cover the wavelength range of interest, one for λ 3400–5200 and the other for 5600–7400 Å. The half width resolution was of 6–7 Å for both settings.

We centered the slits in the brightest parts of the objects. Each object was observed alternating the two slits. Measurements of the sky were obtained at the same time with the other slit. Each beam was treated independently and in all cases the sky was subtracted from the source. The sensitivity of the system for all wavelengths was determined primarily from measurements of standard stars. In addition some PN and H II regions observed with single channel scanners were used as secondary standards. The calibration was derived from standard star fluxes by Stone (1974) and Oke (1974) modified by means of the calibration by Hayes and Latham (1975). The continuum contribution to each emission line was subtracted by interpolating the continuum at both sides of the emission line.

In Table 1 we present the intrinsic line intensities in $\text{erg cm}^{-2} \text{ s}^{-1}$, $I(\lambda)$, given by

$$\log I(\lambda)/I(\text{H}\beta) = \log F(\lambda)/F(\text{H}\beta) + C(\text{H}\beta)f(\lambda) \quad (1)$$

where $F(\lambda)$ is the observed line flux corrected for atmospheric extinction and $C(\text{H}\beta)$ is the logarithmic reddening correction at H β . The reddening function, $f(\lambda)$, normalized at H β is derived from the normal extinction law (Whitford, 1958) and is also presented in Table 1. $C(\text{H}\beta)$ was determined by fitting the observed Balmer decrement, with the exception of H α , to the one computed by Brocklehurst (1971) for $T_e = 10,000^\circ \text{ K}$ and $N_e = 10,000 \text{ cm}^{-3}$. The H α /H β ratio was adjusted to the theoretical one by correcting $F(\text{H}\alpha)$ according to Eq. (1) and by an additional gray shift which was applied to all the lines in the 5600–7400 Å range. This gray shift was always smaller than 0.10 in the log and is due to slight shifts of the observed position and/or changes in seeing conditions from night to night since in many cases the H II regions are bigger than the size of the entrance slit. The resulting accuracy of the blue to red line intensity ratios for bright lines is smaller than 0.05 in the log as can be tested by comparing the theoretical and observed He I (4472/5876) line intensity ratios.

The H and He emission lines are not corrected for underlying absorption due to the following reasons: a) the relatively high dispersions and narrow entrance slit used yield a high emission line to continuum ratio, and b) the effect of the underlying absorption is higher for the fainter emission lines; therefore we can compare the ratios of strong and weak lines of the same element to see if there is a systematic effect; in the case of H with the exception of the high Balmer lines of II Zw 70 we did not detect a systematic effect and in the case of He the 4472/5876 ratios were very close to the theoretical ones indicating that no substantial underlying absorption was present in λ 4472, alternatively

Table 1. Absolute line intensities and reddening corrections; the line intensities are given in $\log I(\lambda)/I(\text{H}\beta)$, $f(\lambda)$ is the reddening function, $C(\text{H}\beta)$ is the logarithmic reddening correction, and $I(\text{H}\beta)$ is the logarithm of the intrinsic flux in $\text{erg cm}^{-2} \text{s}^{-1}$

	Ident.	$f(\lambda)$	NGC 4449 39	NGC 6822 V	NGC 6822 X	IC 10 1	IC 10 2	II Zw 70	II Zw 40	I Zw 18
3727	[OII]	+0.315	+ 0.48	+ 0.16	+ 0.30	+ 0.17	+ 0.16	+ 0.49	+ 0.05	− 0.42
3798	H 10	+0.290	- ...	− 1.30
3835	H 9	+0.280	− 1.14	− 1.12	− 1.18
3869	[NeIII]	+0.270	− 0.61	− 0.38	− 0.44	− 0.63	− 0.44	− 0.41	− 0.20	− 0.71
3889	HeI+H 8	+0.265	− 0.70	− 0.68	− 0.65	− 0.76	− 0.76	− 0.85 ^a	− 0.70	− 0.75
3967+3970	[NeIII]+H 7	+0.235	− 0.65	− 0.56	− 0.57	− 0.68	− 0.58	− 0.68 ^a	− 0.46	− 0.68
4026	HeI	+0.225	...	− 1.71
4068+4076	[SII]	+0.210	− 1.80	− 1.98:
4102	H δ	+0.200	− 0.59	− 0.60	− 0.59	− 0.56	− 0.62	− 0.64 ^a	− 0.61	− 0.58
4340	H γ	+0.135	− 0.33	− 0.32	− 0.31	− 0.34	− 0.31	− 0.33	− 0.27	− 0.32
4363	[OIII]	+0.130	− 1.77	− 1.28	− 1.39	− 1.40:	− 1.36:	− 1.25	− 0.93	− 1.13
4472	HeI	+0.105	− 1.46	− 1.43	− 1.37	...	− 1.40:	− 1.50	− 1.38:	− 1.38:
4658	[FeIII]	+0.050	− 2.10	− 2.00:	− 1.75
4686	HeII	+0.045	− 1.98	< − 2.26	≤ − 2.00	< − 1.80	< − 1.97	− 1.62	< − 1.68	< − 1.4
4713	[ArIV]+HeI	+0.035	...	− 2.02:
4861	H β	+0.000	+ 0.00	+ 0.00	+ 0.00	+ 0.00	+ 0.00	+ 0.00	+ 0.00	+ 0.00
4921	HeI	−0.015	− 2.15	− 1.95
4959	[OIII]	−0.020	+ 0.06	+ 0.26	+ 0.20	+ 0.10	+ 0.25	+ 0.12	+ 0.39	− 0.16
5007	[OIII]	−0.030	+ 0.56	+ 0.73	+ 0.69	+ 0.58	+ 0.73	+ 0.62	+ 0.88	+ 0.33
5198+5200	[NI]	−0.075	− 2.40:
5876	HeI	−0.210	− 1.02	− 0.97	− 0.95	− 1.00	− 1.02	− 1.01	− 1.09	− 1.06
6300	[OI]	−0.285	− 1.61	− 1.97	− 1.48	− 1.62	...
6311	[SIII]	−0.290	− 2.03	− 1.86	− 1.65	− 1.69
6363	[OI]	−0.300	− 2.10	− 2.15	...
6563	H α	−0.335	+ 0.45	+ 0.45	+ 0.45	+ 0.45	+ 0.45	+ 0.45	+ 0.45	+ 0.45
6584	[NII]	−0.340	− 0.83	− 1.21	− 1.23	− 0.97	− 0.94	− 0.88	− 1.14	< − 1.3
6678	HeI	−0.360	− 1.62	− 1.60	− 1.65:	− 1.60	− 1.57	− 1.66:	− 1.58	...
6717	[SII]	−0.370	− 0.84	− 1.20	− 1.11	− 0.99	− 1.05	− 0.71	− 1.25	− 0.97
6731	[SII]	−0.370	− 0.98	− 1.35	− 1.37	− 1.14	− 1.19	− 0.81	− 1.33	...
7065	HeI	−0.400	− 1.83	− 1.68	− 1.46	− 1.74	− 1.43:	...
7136	[ArIII]	−0.410	− 1.17	− 1.06	− 1.02	− 1.01	− 0.93	− 1.22	− 1.19	...
7320+7330	[OII]	−0.435	− 1.49	− 1.66	...	− 1.49::	...	− 1.33
$C(\text{H}\beta)$			0.6	0.8	0.8	1.2	1.5	0.5	1.1	0.1
$I(\text{H}\beta)$			−12.35	−12.05	12.56	−12.47	−12.16	−12.87	−12.29	−13.68

^a Underlying absorption present

the 6678/5876 ratios were smaller than the theoretical ones possibly indicating the presence of some underlying absorption in λ 6678 but other explanations for this result are also possible.

The standard error of estimate in the logarithm between the intrinsic line ratios H 9/H β , H γ /H β , and 4472/5876 presented in Table 1 and the theoretical ones computed by Brocklehurst (1971, 1972) are 0.03, 0.02, 0.02 and 0.03, respectively (observations with a colon not included). The standard errors for the other line intensity ratios have been estimated by comparing results of different nights and for all cases are smaller than 0.05 in the logarithm, with the exception of those lines marked with a colon.

Some of the objects presented in Table 1 have been observed previously (Peimbert and Spinrad, 1970a, b; Searle and Sargent, 1972; Smith, 1975; O'Connell et al., 1978). Our set of data is in

good agreement with previous observations, particularly for strong lines, and comprises a larger number of lines for those objects in common with other observers.

III. Chemical Compositions

1. Temperatures and Densities

The relevant references to the atomic parameters used to derive electron temperatures, electron densities and chemical abundances are those used by Peimbert and Torres-Peimbert (1977) and Torres-Peimbert and Peimbert (1977) with the exception of the newer values for the collision strengths for S⁺ computed by Pradhan (1978).

Table 2. Temperatures, densities, and ionic abundances (log H=12)

	NGC 4449	NGC 6822 <i>V</i>	NGC 6822 <i>X</i>	IC 10 1	IC 10 2	II Zw 70	II Zw 40	I Zw 18
$T(\text{O III})$	9,900	11,200	10,700	11,600	10,600	12,700	13,300	19,600
$\log N_e (\text{S II})$	1.8	<1.4	<1.5	1.6	1.6	2.1	2.5	...
$\log N_e (\text{rms})$	1.0	1.6	1.4	1.1	1.2	0.5	0.4	0.2
$N(\text{He}^+)/N(\text{H}^+)$	0.069	0.076	0.078	0.073	0.073	0.069	0.072	0.074
$N(\text{He}^{++})/N(\text{H}^+)$	0.001	<0.001	<0.001	<0.001	<0.001	0.002	<0.002	<0.003
$\log \text{O}^+$	8.17	7.62	7.85	7.60	7.78	7.75	7.25	6.23
$\log \text{O}^{++}$	8.28	8.25	8.28	8.04	8.34	7.94	8.14	7.13
$\log \text{N}^+$	6.57	6.04	6.07	6.24	6.38	6.23	5.91	<5.40
$\log \text{Ne}^{++}$	7.61	7.59	7.62	7.26	7.64	7.33	7.47	6.44
$\log \text{S}^+$	5.83	5.31	5.41	5.48	5.53	5.68	5.14	4.80
$\log \text{S}^{++}$	6.49	6.42	6.73	6.37
$\log \text{Ar}^{++}$	5.94	5.90	5.99	5.91	6.09	5.60	5.59	...

Table 3. Total abundances. t^2 is the mean square temperature fluctuation, $\log \text{O} = 12 + \log N(\text{O})/N(\text{H})$, $\log \text{X}/\text{O} = \log N(\text{X})/N(\text{O})$, Y and Z are abundances by mass

	NGC 4449 39	NGC 6822 <i>V</i>	NGC 6822 <i>X</i>	IC 10 1	IC 10 2	II Zw 70	II Zw 40	I Zw 18
$t^2 = 0.035$								
$N(\text{He})/N(\text{H})$	0.085	0.081	0.084	0.081	0.078	0.084	0.074	0.076
$\log \text{O}$	8.54	8.34	8.42	8.17	8.45	8.17	8.19	7.18
$\log \text{N}/\text{O}$	-1.60	-1.58	-1.78	-1.36	-1.40	-1.52	-1.34	<-0.83
$\log \text{Ne}/\text{O}$	-0.67	-0.66	-0.66	-0.78	-0.70	-0.61	-0.67	-0.69
X	0.251	0.243	0.250	0.244	0.236	0.250	0.227	0.233
Z	0.0091	0.0058	0.0069	0.0039	0.0075	0.0039	0.0041	0.0004
$t^2 = 0.0$								
$\log \text{O}$	8.38	8.20	8.27	8.04	8.29	8.07	8.09	7.12
$\log \text{N}/\text{O}$	-1.65	-1.67	-1.77	-1.37	-1.40	-1.57	-1.34	<-0.84
Z	0.0063	0.0042	0.0049	0.0029	0.0052	0.0031	0.0033	0.0004

In Table 2 we present the temperature derived from the [O III] lines, $T(\text{O III})$, which is density-independent for these objects and the density derived from the [S II] lines which is temperature-independent and that usually arises from regions with higher density than the average. Logarithmic errors of 0.05 in the line intensity ratio yield errors of 450° K at 10,000° K, and 1100° K at 20,000° K, and correspond to uncertainties of 0.06 in $\log \text{O}^{++}$.

The root mean square density, $N_e(\text{rms})$, was determined as follows. The intrinsic $\text{H}\beta$ flux observed from a homogeneous sphere of radius r is given by

$$I(\text{H}\beta) = \frac{N_e(\text{rms}) N_p(\text{rms}) r^3 a(4 \rightarrow 2, T) h\nu(4 \rightarrow 2)}{3d^2}, \quad (2)$$

where $a(4 \rightarrow 2, T)$ is the $\text{H}\beta$ effective recombination coefficient, d is the distance to the object and N_e and N_p are the electron and proton densities. From (2) we have

$$N_e^2(\text{rms}) = \frac{3d^2 I(\text{H}\beta) \left[1 + \frac{N(\text{He}^+)}{N(\text{H}^+)} + \frac{2N(\text{He}^{++})}{N(\text{H}^+)} \right]}{r^3 a(4 \rightarrow 2, T) h\nu(4 \rightarrow 2)}. \quad (3)$$

To derive the $N_e(\text{rms})$ values given in Table 2 we assumed that our observations were representative of a spherical core with

$r = 3''9$, which corresponds to the area of our rectangular entrance slit, and used Eq. (3) with the distances in Table 5, the helium abundances in Table 3, the $I(\text{H}\beta)$ values of Table 1 and the $a(4 \rightarrow 2, T)$ value for $T_e = 10,000^\circ \text{K}$ by Brocklehurst (1971).

2. Chemical Abundances

The ionic chemical abundances were derived assuming for the mean-square temperature fluctuation, t^2 , a value of 0.035 (Peimbert and Torres-Peimbert, 1977) and are presented in Table 2. We do not have enough information to specify the t^2 value for each object. The real t^2 value is expected from theoretical models to be somewhere in the $0.01 < t^2 < 0.04$ range; the higher values corresponding to H II complexes made of unconnected H II regions ionized by stars of different temperatures. Fortunately, an error of 0.02 in t^2 will produce an error of less than 0.01 in $\log N(\text{He})/N(\text{H})$ and of less than 0.1 in $\log N(\text{X})/N(\text{H})$, where $N(\text{X})$ denotes an abundance derived from a forbidden line. To produce a direct estimate of the errors introduced by using a different t^2 value we have also computed the chemical abundances for $t^2 = 0.00$ which is the case of uniform temperature along the line of sight. In all figures and discussions we have adopted the abundance values for $t^2 = 0.035$.

Table 4. Abundances of the Magellanic Clouds, Orion, and the Sun ($\log H = 12$)^a

t^2	SMC		LMC		Orion	Sun
	0.035	0.00	0.035	0.00	0.035	...
log O	7.99 \pm 0.08	7.89	8.50 \pm 0.08	8.34	8.75 \pm 0.08	8.92
log N/O	-1.50 \pm 0.07	-1.48	-1.29 \pm 0.07	-1.31	-0.99 \pm 0.07	-0.93
log Ne/O	-0.86 \pm 0.13	-0.86	-0.86 \pm 0.14	-0.90	-0.85 \pm 0.07	-0.80
log S/O	-1.55	-1.69
Y	0.237 \pm 0.002	0.237	0.249 \pm 0.005	0.250	0.280 \pm 0.010	...
Z	0.0026	0.0021	0.0083	0.0057	0.014–0.019	0.021:
	(a)		(b)		(c)	(d)

^a Standard deviations were obtained from the values for different regions

(a) Observational data from Peimbert and Torres-Peimbert (1976), abundances rederived here

(b) Observational data from Peimbert and Torres-Peimbert (1974), abundances rederived here

(c) Peimbert and Torres-Peimbert (1977), Pagel (1978)

(d) Lambert (1978), Bertsch et al. (1972), Lambert and Luck (1978)

The total O, N, and Ne abundances were obtained from

$$\frac{N(O)}{N(H)} = \frac{N(He^{++} + He^+)}{N(He^+)} \frac{N(O^+ + O^{++})}{N(H^+)}, \quad (4)$$

$$\frac{N(N)}{N(H)} = \frac{N(O)}{N(O^+)} \frac{N(N^+)}{N(H^+)}, \quad (5)$$

$$\frac{N(Ne)}{N(H)} = \frac{N(O)}{N(O^{++})} \frac{N(Ne^{++})}{N(H^+)}, \quad (6)$$

and are presented in Table 3.

The He/H abundance ratio is given by

$$\frac{N(He)}{N(H)} = \frac{N(He^0 + He^+ + He^{++})}{N(H^+)}. \quad (7)$$

The $N(He^+)/N(H^+)$ abundance ratio was derived from the 4472, 5876, and 6678 to H β ratios giving them relative weights of 1, 2, and 1, respectively, due to their relative intensities. We have also considered the effect of self-absorption. The ionization potentials of S, O, and He, in general imply that $N(S^+)/N(S) < N(He^0)/N(He) < N(O^+)/N(O)$, therefore it has been proposed that

$$\begin{aligned} \frac{N(He^0 + He^+)}{N(H^+)} &= i_{cf}(He) \frac{N(He^+)}{N(H^+)} \\ &= \frac{1}{1 - \gamma [N(O^+)/N(O)] - (1 - \gamma) [N(S^+)/N(S)]} \\ &\quad \cdot \frac{N(He^+)}{N(H^+)}, \end{aligned} \quad (8)$$

for $0 \leq \gamma \leq 1$. In this relation γ is adjusted to yield the smallest dispersion of $N(He)/N(H)$ ratios for all the observed regions of a given nebula. The value of γ depends on the density distribution (Peimbert et al., 1974) and has to be determined for each object. For the Orion nebula $\gamma = 0.35$ (Peimbert and Torres-Peimbert, 1977) and for the Carina nebula $\gamma = 0.20$ (Peimbert et al., 1978). The electron densities of the objects under consideration are smaller than those of Orion and the Carina nebula, therefore based on ionization models for densities in the 10–100 cm⁻³ range (Peimbert et al., 1974) we adopted $\gamma = 0.15$. For the two objects with the lowest O⁺/O ratio, I Zw 18 and I Zw 40, and again based on ionization models we adopted the ionization cor-

rection factor given by

$$i_{cf}(He) = 1/[1 - 0.25 N(O^+)/N(O)]. \quad (9)$$

From Eqs. (7)–(9) the total He/H abundance ratios presented in Table 3 were derived. For the S⁺/S determination we assumed $\log N(S)/N(O) = -1.55$ for all the observed objects (Peimbert and Torres-Peimbert, 1977; Pagel, 1978).

The use of Eqs. (8) and (9) might introduce a systematic error in the He/H abundance ratios due to a weak correlation between O⁺/O and Z in the sense that the higher the oxygen ionization degree the lower the oxygen abundance. This correlation factor is smaller, yielding a more accurate He/H abundance ratio, for the objects of higher degree of ionization and lower metallicity than those of lower degree of ionization and higher metallicity. This problem does not affect the SMC and LMC He/H values because they were not derived from equations of the type of (8) and (9) but from the $N(He^+)/N(H^+)$ vs $N(O^+)/N(O^+ + O^{++})$ diagram (Peimbert and Torres-Peimbert, 1976). The similar results derived from the Magellanic Clouds and the objects presented in this paper imply that any systematic error due to the ionization degree, if present, is very small.

The heavy element abundance, Z, was obtained by assuming it to be proportional to the oxygen abundance and that for $\log N(O)/N(H) = -3.42$, $Z = 0.01$, i.e. that O constitutes 45% of Z by mass (Peimbert and Torres-Peimbert, 1974). The Y and Z values are presented in Table 3. Also in Table 3 we present the abundances for $t^2 = 0.00$. The Y value is practically independent of the adopted t^2 value.

We decided to add to our discussion the results for the Magellanic Clouds' H II regions. There is good agreement from the recent observations of these objects (Peimbert and Torres-Peimbert, 1974, 1976; Dufour, 1975; Dufour and Harlow, 1977; Dufour and Killen, 1977; Aller et al., 1977; Pagel et al., 1978); for the following discussion we will use the observations by Peimbert and Torres-Peimbert (1974, 1976) which are particularly accurate for the determination of the He/H abundance ratio. We recomputed the abundances of the Magellanic Clouds to have them in a homogeneous system; the changes with respect to the previous values are due to: a) for the LMC, the newer cross sections for the [O III] lines derived by Seaton (1975) and b) for both clouds, the smaller value for t^2 . The average values

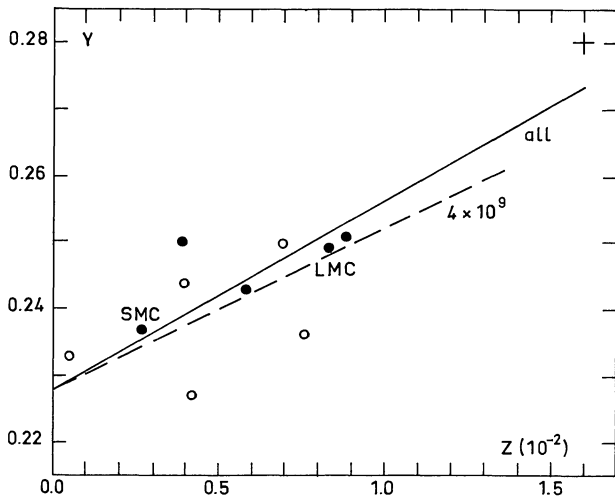


Fig. 2. Comparison between observed helium and heavy element abundance by mass. *Solid line*, the least-squares solution for all objects. *Dashed line*, model with mass loss, for $t_c = 4 \times 10^9$ yr. Filled circles are higher quality observations, the cross corresponds to the Orion Nebula

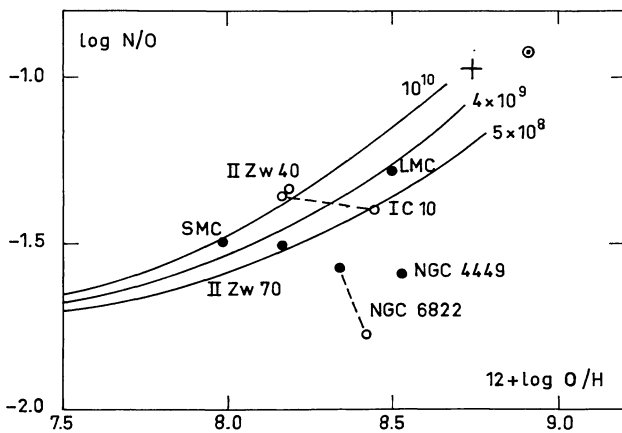


Fig. 3. Observed N/O vs. O/H ratio for all objects. Filled circles are higher quality observations. *Solid lines*, are models with mass loss for values of t_c of 5×10^8 , 4×10^9 , and 1×10^{10} yr. We have indicated the values for the Orion nebula (marked with a cross) and the Sun. Extrapolation of the models to the region of these points would make no sense

for the six regions in the LMC and for the four regions in the SMC are presented in Table 4, together with the abundances for the Orion nebula and the Sun.

3. Pregalactic Helium Abundance and the Helium Enrichment

In Fig. 2 we present the Y vs Z plot for our sample where we have added the value for the Orion nebula for $Z = 0.016$. The best values are those for the Magellanic Clouds, due to the large number of regions observed in each cloud and to the very small neutral helium correction and for the Orion nebula due to the high quality of the line intensity measurements and the large number of regions observed.

Since the galaxies with the largest gas to total mass ratio, $M_{\text{gas}}/M_{\text{tot}}$, are those with the lowest values of Z it follows that the heavy elements are due to the enrichment of the interstellar medium by stellar evolution processes. Consequently, the value of Y for $Z=0$ corresponds to the pregalactic helium abundance, Y_p , and for big-bang cosmologies to the primeval helium abundance. From stellar evolution theory it is assumed that all Z and the additional Y are mainly produced by stars with $M > 3 M_{\odot}$; therefore the deviations from instant recycling are only moderate and it is reasonable to make a linear fit to derive Y_p and the helium to heavy elements enrichment ratio $\Delta Y/\Delta Z \equiv (Y - Y_p)/Z$ (e.g. Sects. V, VI; Chiosi, 1978; Serrano and Peimbert, 1979).

Elsewhere a detailed discussion of the helium enrichment based on planetary nebulae data is presented (Serrano and Peimbert, 1979).

Least-square fits giving equal weight to each galaxy yield the following coefficients and standard deviations:

- $Y = (0.228 \pm 0.004) + (2.83 \pm 0.60)Z$ for all galaxies and Orion
- $Y = (0.233 \pm 0.005) + (1.73 \pm 0.90)Z$ for all galaxies without Orion
- $Y = 0.231 + 2.11 Z$ for the SMC and the LMC.

These results imply that the pregalactic helium abundances derived from the Magellanic Clouds and from the objects presented here are in excellent agreement. The standard error includes the observational errors of random nature but not the systematic errors. There are at least five sources of systematic errors: i) the atomic parameters, ii) the relative photometric calibration, iii) the value of t^2 , iv) the helium underlying absorption and v) the correction for neutral helium. The expected error due to the atomic parameters is at most of a few per cent (Seaton, private communication, 1974); an error of 3% in the He/H effective recombination coefficients ratio amounts to 0.006 in Y_p . The relative photometric calibration is expected to be correct within 1–2% in the wavelength range of interest (Hayes and Latham, 1975). As discussed above, the effect of t^2 in the He/H ratio is negligible and the correction due to helium underlying absorption as well as the error due to the correction for neutral helium are small. From the previous discussion we think that a 3σ error yields a realistic estimate of the pregalactic helium uncertainty; therefore it follows that $Y_p = 0.228 \pm 0.014$.

4. Nitrogen to Oxygen Enrichment Ratio

A relationship of the type $[N/O] = a[O/H]$ with $a = 1$ is predicted by simple models with instant recycling approximation assuming nitrogen to be of secondary origin (Talbot and Arnett, 1973). Smith (1975) from observations of extragalactic H II regions in M 33 and M 101 found that $a \sim 0.5$ implying a primary origin for part of the nitrogen. Peimbert (1978b) from recent observations of galactic H II regions obtained $a = 0.4 \pm 0.2$. Alloin et al. (1979) and Edmunds and Pagel (1978) from analyses of H II regions in several galaxies also reach the conclusion that a substantial fraction of nitrogen is of primary origin. Edmunds and Pagel suggest that N is produced by stars in the $1\text{--}2.5 M_{\odot}$ range; planetary nebulae of Type I seem to be responsible for some primary production of N in agreement with this suggestion; on the other hand the abundances of planetary nebulae of Type II are consistent with secondary production of N (Peimbert, 1978a).

In Fig. 3 we present the N/O vs. O/H plot for our objects. A linear fit for the SMC and the LMC yields $a = 0.4$, while for

Table 5. Masses and luminosities

Galaxy	Adopted distance (Mpc)	R	$M_{\text{gas}}(R)$ (M_{\odot})	$M_{\text{tot}}(R)$ (M_{\odot})	$M_{\text{gas}}/M_{\text{tot}}$	M_{tot}/L_B^0 ($M_{\odot}/L_{B\odot}$)	Notes
NGC 4449	5.0:	0°4	$6.0 \cdot 10^9$	$4 \cdot 10^{10}$:	0.15:	6.5:	a
NGC 6822	0.6	18'	$1.9 \cdot 10^8$	$1.7 \cdot 10^9$	0.11	9.4	b
IC 10	3.0	5'	$1.3 \cdot 10^9$	$5.4 \cdot 10^9$	0.24:	3.7:	c
II Zw 70	19	1°5	$3.8 \cdot 10^8$	$1.3 \cdot 10^9$	0.29	1.1	d
II Zw 40	9.7	1°1	$2.5 \cdot 10^8$	$\geq 7.4 \cdot 10^8$	≤ 0.34 :	≤ 1.5	e
I Zw 18	12	...	$1.2 \cdot 10^8$	f
SMC	0.070	2°5	$6.3 \cdot 10^8$	$1.5 \cdot 10^9$	0.42	1.5:	g
LMC	0.052	4°2	$7.1 \cdot 10^8$	$6.1 \cdot 10^9$	0.12	1.6:	h

Notes:

 R is the radius where $M_{\text{gas}}/M_{\text{tot}}$ is known L_B^0 is from de Vaucouleurs et al. (1976) for all galaxies

a van Woerden et al. (1975). Distance of C Vn I group from Sandage and Tammann (1975)

b Gottesman and Weliachew (1977); distance is a compromise between various determinations

c Shostak (1974). Distance from Sandage and Tammann (1975)

d Balkowski et al. (1978). Distance from redshift with $H=70 \text{ km s}^{-1} \text{ Mpc}^{-1}$. O'Connell et al. (1978) give a mass of gas 1.6 times highere M_{gas} and M_{tot} for core (Gottesman and Weliachew, 1972). Distance from redshift with $H=70 \text{ km s}^{-1} \text{ Mpc}^{-1}$ f Chamaraux (1977). Distance from redshift with $H=70 \text{ km s}^{-1} \text{ Mpc}^{-1}$ g Hindman (1967). M_{tot}/L_B^0 may be underestimated by a factor $\simeq 3$ (see Lequeux, 1979)h McGee and Milton (1966). M_{tot}/L_B^0 may be underestimated by a factor $\simeq 3$ (see Lequeux, 1979)

the five best observed objects (without Orion) yields $a=0.1$. The diagram shows considerable scatter with respect to a simple behaviour between both quantities; part of the scatter could be due to observational errors, particularly since any error in the electron temperature would displace the object in a transverse direction to that established by the best observed objects i.e. a higher temperature corresponds to a smaller O/H and a higher N/O ratio. A primary production of $\log \text{N/O} < -1.5$ seems indicated by the data. Figure 3 will be discussed again in Sect. V. It is clear that more observations are needed to find out if the scatter is real or if it is due to observational errors. The theoretical results by Weaver et al. (1978) on the presupernova evolution of objects with $15 M_{\odot}$ and $25 M_{\odot}$ are consistent with a modest primary production of nitrogen in agreement with our observations.

IV. Masses, Z vs. M_{tot} Relation, and Yields

1. Gaseous and Total Masses

An interesting quantity to consider in the study of evolution of galaxies is the mass of gas to total mass ratio, $M_{\text{gas}}/M_{\text{tot}}$. This ratio is an index of the stage of evolution of galaxies: the more evolved objects have had more gas transformed into stars, and thus a lower gas to total mass ratio.

The atomic hydrogen mass, M_{H} , can be derived for the galaxies of the present work from published 21-cm line observations and assuming the distance to each object. To take helium into account we assume $M_{\text{gas}}=1.3 M_{\text{H}}$. We have not considered molecular hydrogen, because it is not likely to be present in large proportions since these galaxies do not contain much dust, and it is thought that molecular hydrogen is formed on grains.

Total masses are also known with relatively good accuracy for those galaxies which have been mapped in the 21-cm line and for which a rotation curve has been obtained. This is the case for most of the galaxies in our program, except I Zw 18 for which the total mass is unknown. We have estimated $M_{\text{gas}}/M_{\text{tot}}$ in the part of the galaxy where the rotation curve, thus the total mass is known. This corresponds to most of the galaxy except for II Zw 40 where the studied region is the hydrogen core only, with radius $R=1'1$. The total mass for NGC 4449 has been calculated from preliminary data published by van Woerden et al. (1975) but is somewhat uncertain. Table 5 displays the results and corresponding references as well as the M_{H}/L_B^0 ratios.

2. Heavy Element Enrichment vs. M_{tot}

We decided to test whether the trend found for members of the local group and for elliptical galaxies, in the sense that the higher the total mass the higher the heavy element content (e.g. van den Bergh, 1968; Peimbert and Spinrad, 1970b; Faber, 1973), applies to the interstellar matter of the objects presented here.

In Fig. 4 we plot the Z vs. M_{tot} for the galaxies under consideration. As discussed above for I Zw 18 and II Zw 40 we only have lower limits for M_{tot} (that for I Zw 18 is simply M_{gas}). For II Zw 40 we have added to the value in Table 5 the mass of gas of the outer halo ($2.5 \cdot 10^8 M_{\odot}$, Gottesman and Weliachew, 1972). We think that the lower limit for I Zw 18 should be very close to the total value because this object shows a very small heavy element abundance indicating that most of its mass should be in gaseous form. Figure 4 shows a very strong correlation between M_{tot} and Z which can be adjusted by a linear relation

$$\log M_{\text{tot}} = b + cZ. \quad (10)$$

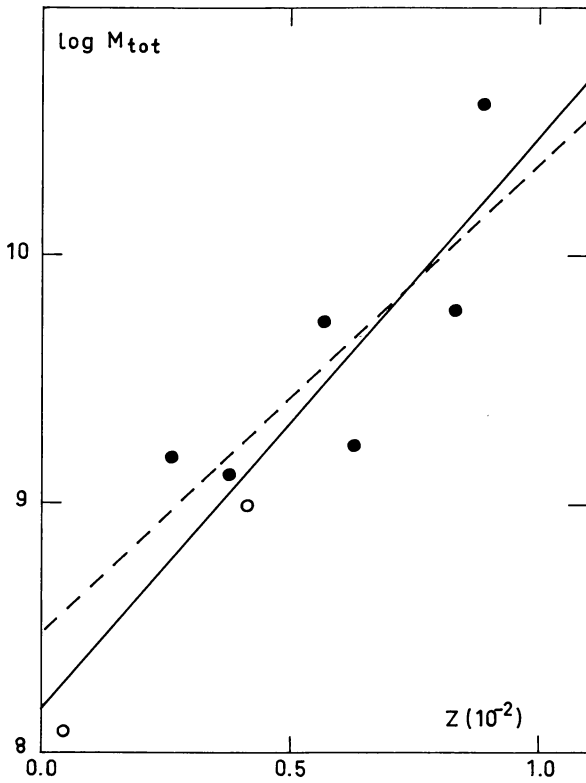


Fig. 4. Observed heavy element abundance, Z , versus total mass for the compact and irregular galaxies under consideration. Filled circles are objects with known mass; open circles are lower limits to the total mass for I Zw 18 and II Zw 40 (for which we adopted $9.9 \cdot 10^8 M_{\odot}$). *Solid line*, least-squares fit for all galaxies ($\log M_{\text{tot}} = 8.18 + 229 Z$). *Dashed line*, least-squares fit for galaxies of known mass ($\log M_{\text{tot}} = 8.48 + 187 Z$)

The coefficients and standard deviations are $b = 8.18 \pm 0.24$ and $c = 229 \pm 43$ when all objects are considered, or $b = 8.48 \pm 0.41$ and $c = 187 \pm 64$ without considering I Zw 18 and II Zw 40. (M_{tot} is given in solar units). This correlation seems to be caused by the lower $M_{\text{gas}}/M_{\text{tot}}$ ratio present in the more massive objects (see Sect. IV.1) which apparently indicates that averaged over the whole history of a galaxy the process of star formation is more efficient in the most massive ones.

3. Observed and Theoretical Yields

In relatively unevolved systems, like the ones we are considering, there should be a single monotonic relation between the abundance of primary elements and $M_{\text{gas}}/M_{\text{tot}}$. This statement is valid when: a) galaxies evolve as closed, well mixed systems, b) the instantaneous recycling approximation applies, and c) the IMF and nucleosynthesis are the same for all systems. Since primary elements are thought to be formed in massive stars, condition (b) should be true for these elements independently of the details of star formation. Under these assumptions

$$Z = p \ln (M_{\text{tot}}/M_{\text{gas}}) \quad (11)$$

where the heavy element yield, p , is defined as the ratio of heavy elements newly synthesized and ejected to the mass locked up in stars and stellar remnants per generation of stars. This quantity

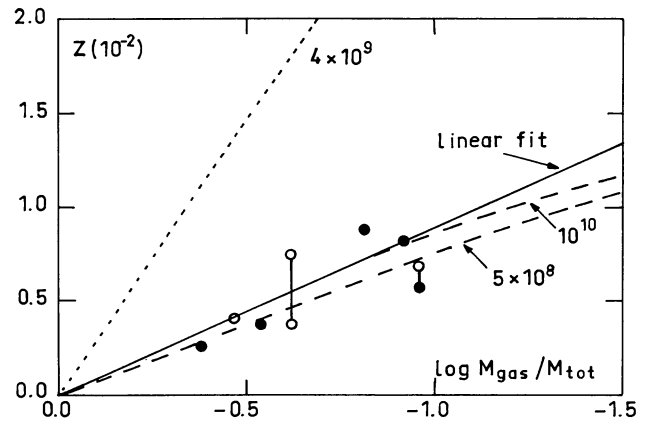


Fig. 5. Heavy element abundance versus gas mass to total mass ratio. *Solid line* is the least-squares fit to the observations $Z = -0.0003 + 0.0039 \ln (M_{\text{tot}}/M_{\text{gas}})$. *Dashed lines* are model calculations for extreme mass loss and different rates of star formation. *Dotted lines* is model calculation for no mass loss. For each model the characteristic time is indicated. Symbols as in Fig. 2 and 3

Table 6. Heavy element yields

p	
Observational	Theoretical
0.004 ± 0.001 ^a	0.004 ^e
0.004 ^b	0.013 ^f
0.003 ^c	$0.002 - 0.010$ ^g
0.005 ± 0.001 ^d	$0.011 - 0.034$ ^h
	> 0.015 ⁱ

- a This work. For the irregular and blue compact galaxies in our sample.
b Pagel (1978) from the gradient of oxygen in the galaxy.
c Pagel et al. (1978) from SMC and LMC H II regions.
d Pagel and Patchett (1975) from the average metallicity of stars in the solar neighborhood.
e This work. IMF given in Sect. V.1, and extreme mass loss models by Chiosi et al., $\alpha = 0.9$.
f This work. IMF given in Sect. V.1, and no mass loss.
g Chiosi and Caimmi (1979) from Arnett's computations for an IMF slope of $7/3 - 4/3$ and allow for mass loss (with their parameter $\alpha = 0.9$).
h Arnett (1978) from evolutionary models of helium stars and for an IMF slope between $7/3$ and $4/3$.
i Thuan et al. (1975) from stellar models by Talbot and Arnett (1971) and adjusting the IMF to fit the observed luminosity function in the solar neighborhood.

depends only on stellar nucleosynthesis and the IMF. Thus a linear relation with slope p is expected between the abundance of primary elements and $\ln (M_{\text{tot}}/M_{\text{gas}})$.

A linear least square fit for the galaxies in our sample yields

$$Z/10^{-2} = (-0.03 \pm 0.16) + (0.39 \pm 0.10) \ln (M_{\text{tot}}/M_{\text{gas}}), \quad (12)$$

where we have included standard deviations. The linear fit to the observations is consistent with the assumptions used to derive

Eq. (11), since for $M_{\text{gas}} = M_{\text{tot}}$, i.e. pregalactic conditions, Z is zero and thus we obtain from our data a yield of $p = 0.004 \pm 0.001$. In Fig. 5 we present the empirical Z and $M_{\text{gas}}/M_{\text{tot}}$, as well as the regression line.

In Table 6 we present the observed and theoretical yields from other authors. The theoretical yields computed by Arnett (1978) without mass loss and for an IMF given by a power law with a slope between $4/3$ and $7/3$ are considerably higher than the observations. The yields computed by Chiosi and Caimmi (1978), based on nucleosynthesis computations by Arnett and mass loss models by Chiosi et al. (1978) with the mass loss parameter $\alpha = 0.90$, and a power law IMF with a slope of 2 are in excellent agreement with our observations. Yields derived from models without mass loss and reasonable initial mass functions fail to agree with our observations.

V. Model Calculations of Chemical Evolution of Irregular Galaxies

To gain further insight from our observations we have carried out model computations. We have used an improved version of the chemical evolution programs developed by Vigroux et al. (1976) as described by Alloin et al. (1979) combined with that of Serrano (1978). Major changes with respect to these programs are presented in 1, 2, and 3, while in 4 we discuss other characteristics in common with previous works.

1. New Initial Mass Function, IMF

We have assumed that the IMF is independent of time and is given by

$$\psi(M) dM = \frac{MB(M, t) dM}{\int MB(M, t) dM} \quad (13)$$

with $\int \psi(M) dM = 1$

where $B(M, t)$ is the rate of star formation per unit mass.

The high mass part of this IMF ($M > 2.5 M_{\odot}$) has been derived independently by Lequeux (1979) and Serrano (1978). The derivation by Lequeux is based on the CGO catalogue (Cruz-González et al., 1974), the Michigan catalogue (Houck and Cowley, 1975), and the catalogues of B stars by Lesh (1968, 1972); particular attention was paid to completeness, interstellar extinction and runaway stars. Alternatively Serrano has obtained a similar IMF in this mass range by considering: the CGO catalogue (assuming that all the stars are of Population I), the solar neighborhood data by Mc Cuskey (1966) and the luminosity function for open clusters by Taff (1974).

The low mass part of the IMF has been derived by Serrano (1978) from a detailed discussion of the local stellar luminosity function.

We have assumed continuity of the two portions of the IMF at $1.8 M_{\odot}$. We have set the high mass and low mass cut-offs at $110 M_{\odot}$ and $0.007 M_{\odot}$, respectively. With this choice of parameters the luminosity function is given by

$$\begin{aligned} \psi(M) &= 0.56 M^{-2} & \text{for } M \geq 1.8 M_{\odot}, \\ &= 0.25 M^{-0.6} & \text{for } M < 1.8 M_{\odot}. \end{aligned} \quad (14)$$

It should be noted that the slopes of the two sections of the IMF are such that the total rate of transformation of gas is *not* sensitive to either the high mass or the low mass cut-offs. Moreover the

steeper slope of the high mass part of the adopted IMF with respect to that of Salpeter (1955) that has been used by most authors, has important consequences for nucleosynthesis; namely, intermediate mass stars, which have different nucleosynthetic yields from those of high mass stars, play a relatively larger role.

2. Mass Loss by Massive Stars on the Main Sequence

We have computed 2 cases: a) no stellar mass loss and, b) the largest mass loss rate case described by Chiosi (1979), corresponding to $\alpha = 0.9$.¹ As discussed by Chiosi et al. (1978) and by Chiosi and Caimmi (1979), the effect of mass loss during the core H and He-burning phases is to decrease the mass of the helium core with respect to that of stars of the same initial mass without mass loss. This, in turn, changes the yields of heavy elements in the direction of a general decrease. We have adopted for the helium cores the mass given by Chiosi and Caimmi (1979), the final composition of the cores being that given by Arnett (1978), for a given core mass.

3. Nitrogen and Carbon

We have left as free parameters to be determined from comparison with observations: a) the ratio of primary ^{14}N to ^{16}O (in Sect. III we have discussed the observational evidence in favor of primary production of N); b) the rate of secondary production of ^{14}N in the hydrogen and helium zones; and c) the contribution to the ^{12}C abundance by stars in the $5\text{--}10 M_{\odot}$ range since it is possible for the mechanism of thermal pulses and further dredge-up to be responsible for some carbon production in this stellar mass range.

4. Further Aspects of the Program

Other than the changes noted above, we used the element production data by Arnett (1978) for massive stars ($M > 10 M_{\odot}$) and Iben (1977) and Iben and Truran (1978) for less massive stars. We have adopted $Y_p = 0.228$, the result derived in Sect. III.

We have considered closed models, i.e. models without galactic mass loss or infall (constant M_{tot}). We have also considered the delay in the enrichment of the ISM due to the stellar lifetimes, therefore dropping the instantaneous recycling approximation.

In all our models we have adopted

$$\frac{(M_{\text{gas}}/M_{\text{tot}})}{dt} = -\text{SFR} (1 - \beta) \quad (15)$$

where SFR, the star formation rate, is constant in time, and β is the return fraction of mass per stellar generation. In the case of constant SFR it is given by

$$\beta(t) = \frac{M_{\text{max}}}{M(t)} \int f_{ej}(M) \psi(M) dM \quad (16)$$

where M_{max} and $M(t)$ are the high mass cut-off and the stellar mass corresponding to a lifetime t , respectively; and $f_{ej}(M)$ is the fraction of mass ejected for stars of mass M . The characteristic time for each model, $t_c \equiv \text{SFR}^{-1}$, is the time required to have converted into stars a mass M_{tot} .

¹ Although Chiosi (private communication) now favors $\alpha = 0.83$ for the solar neighborhood, he indicates that $\alpha = 0.90$ might be more appropriate for irregular galaxies, whose lower Z might yield an increase of the mass loss.

Table 7. Helium to heavy elements enrichment ratio computed at $M_{\text{gas}}/M_{\text{tot}}=0.1$. Models, other than IRA, are labelled by t_c , also $t(10\%)$ the time needed to deplete $M_{\text{gas}}/M_{\text{tot}}$ to 10% is given

Model $t_c(10^9 \text{ yr})$	$t(10\%)$	$\Delta Y/\Delta Z$	
	t_c	mass loss $\alpha=0.9$	no mass loss
0.5	1.02	2.1	0.5
4	1.14	2.4	0.7
10	1.20	3.2	0.9
IRA	1.28	4.3	1.4

In such models the age of each galaxy, i.e. the epoch when star formation has begun is

$$\tau = t_c [1 - (M_{\text{gas}}/M_{\text{tot}})] / \langle 1 - \beta \rangle, \quad (17)$$

and it is not necessarily the same for all galaxies. No special significance is to be attached to this SFR prescription which may or may not be valid for the studied objects. We have run models with different SFR values, only in order to explore the sensitivity of the abundances to the SFR for a given $M_{\text{gas}}/M_{\text{tot}}$. We discuss the problem of the ages in Sect. VI.4.

VI. Comparison with Observations

In this section we compare the results of our models with the observations. As has been discussed before (e.g. Talbot and Arnett, 1973) the instant recycling approximation, IRA, is valid for objects with large $M_{\text{gas}}/M_{\text{tot}}$ ratio and of ages longer than the main sequence lifetime of the stars expected to contaminate the interstellar medium. We have computed models for t_c ranging from $5 \cdot 10^8$ to 10^{10} yr, the latter ones deviating the least from IRA.

The heavy element yield, which is dominated by the primary elements, and particularly by the O/H ratio, is not affected considerably by deviations from IRA, therefore the results by Arnett (1978), Chiosi and Caimmi (1978), and Thuan et al. (1975) in Table 6 derived under IRA can indeed be compared with the observations. Alternatively departures from IRA affect moderately the $\Delta Y/\Delta Z$ ratio and very considerably the nitrogen and carbon production. This opens in principle a way of solving a major pending question: what is the age of irregular and blue compact galaxies? (Searle et al., 1973).

We will now analyze each possible observable quantity with the model predictions to try to discriminate among possible solutions.

1. Heavy Element Yield

In Fig. 5 we compare the observed Z vs $(M_{\text{gas}}/M_{\text{tot}})$ relation with results of model calculations. As can be seen in this figure the agreement can be reached only for models including mass loss by massive stars during their evolution, while models without mass loss produce too much oxygen. As expected for a primary element in an unevolved system, the abundance of oxygen is insensitive to the past history of star formation. This can be seen by the very small difference between the long lifetime model ($t_c=1 \cdot 10^{10}$ yr) and the short lifetime one ($t_c=5 \cdot 10^8$ yr) which amounts to only $\sim 10\%$ in the O/H ratio. The heavy element

yields that are based on the oxygen yields and on the assumption that 45% of Z is in the form of ^{16}O , are presented in Table 6. It is clear from this table that the derived heavy element yield for our models with mass loss fits the observational data for blue and irregular galaxies.

2. Helium to Heavy Elements Enrichment Ratio, $\Delta Y/\Delta Z$

In Table 7 we present several values for the $\Delta Y/\Delta Z$ ratio for models with and without mass loss. The models with mass loss predict values closer to the observations due to the lower heavy element yield. As can be seen from this table the IRA values are higher than those given by our evolutionary models. The reason is that while the heavy elements are mainly produced by stars with $M > 20 M_{\odot}$ most of the helium is produced by stars in the $3\text{--}10 M_{\odot}$ range. The different main sequence lifetimes of stars of 20 and $3 M_{\odot}$ (approximately 10^7 and $3 \cdot 10^8$ yr respectively) produce two effects not included in IRA: not only a time lag in the Y production relative to the Z production, but also that most stars of all masses are formed with a smaller Y fraction than in IRA and at later times they return matter with Y values smaller than in IRA. The longer t_c , the closer the model is to IRA conditions as can be seen from Table 7.

In Fig. 2 we present the helium to heavy element enrichment ratio derived from a stellar mass loss model of $t_c=4 \cdot 10^9$ yr which is in very good agreement with the observations. Variations in t_c produce changes in the $Y\text{--}Z$ diagram in the sense that for a given Z value, the smaller the t_c value the smaller the Y value. The accuracy of present $Y\text{--}Z$ observations is not high enough to distinguish variations in t_c of less than a factor of five.

3. Nitrogen and Carbon

In order to fit the observed $N(\text{C})/N(\text{O})=0.58$ ratio of the Orion nebula and the Sun (Peimbert and Torres-Peimbert, 1977; Lambert, 1978) it is found that mass loss models with $\alpha=0.9$ would require 22% of the carbon atoms to originate in stars in the $5\text{--}10 M_{\odot}$ range. This means that only 2% of their He zone would be converted into carbon. For the case without mass loss we found that 11% of their He zone would have to be converted into carbon.

The production of carbon by stars in the $5\text{--}10 M_{\odot}$ range is still very uncertain since the carbon yields from massive stars are not very precise and low-mass stars like planetary nebulae seem to be producing carbon (Torres-Peimbert and Peimbert, 1977).

By giving more weight to the SMC and the LMC points in the N/O vs O/H diagram a reasonable fit for the models with mass loss is obtained by adopting: a) a primary abundance ratio of $\log N(\text{N})/N(\text{O}) = -1.7$, and b) secondary ^{14}N produced by combustion of 10% of the initial C in the hydrogen zones, (or any quantitatively equivalent production). Models for three t_c with mass loss are presented in Fig. 3. In the case of models without mass loss a reasonable fit is obtained by adopting: a) a primary ^{14}N production corresponding to $\log N/\text{O} = -1.7$, b) secondary ^{14}N produced by combustion of 32% of the initial C in the hydrogen zones, and of all the C and O initially present in the helium zones.

4. SFR and the M/L Ratio

As shown by Searle et al. (1973) the very blue compact galaxies that we are considering cannot have had a decreasing or even uniform rate of star formation during the last 10^{10} yr. There are two possible models which can account for their colors; either

a) star formation started only recently or, b) star formation may have proceeded for a long time but the present rate of star formation much exceeds the average rate in the past. These conclusions are confirmed and strengthened by more recent works (Huchra, 1977; Larson and Tinsley, 1978). Although the new IMF used in the present work differs appreciably from those used in previous ones, the corresponding changes in color are insufficient to affect these conclusions. For example, preliminary computations with this IMF show that the colors of irregular galaxies ($\langle B-V \rangle \simeq 0.35$, $\langle U-B \rangle \simeq -0.2$) are well reproduced by models of constant SFR of $t_c \simeq 1-4 \cdot 10^9$ yr. Indeed Butcher (1977) has given evidence based upon a study of the luminosity function in a field region of the LMC that the bulk of star formation began $3-5 \cdot 10^9$ yr ago in this galaxy (however this conclusion might have to be modified if the IMF in the LMC is similar to the IMF used here). The colors of the blue compact galaxies would correspond to an even shorter duration of star formation (a "burst"); in this case timescales of 10^7 to a few 10^8 yr are indicated by model calculations. Independent evidences for such a burst in II Zw 70 have been presented by Bergeron (1976) and O'Connell et al. (1978). The only important difference between blue compact and irregular galaxies appears to be their present SFR (see e.g. Balowski et al., 1978). The present burst in blue compact galaxies might well hide an older stellar component formed at a slow average rate, which might be responsible for the bulk of the nucleosynthesis of the heavy elements that we observe in these objects.

If indeed their present SFR is the only difference between blue compact and irregular galaxies, in principle it should be possible to distinguish between the alternatives suggested by Searle et al. (1973) by means of Figs. 2 and 3. If the blue compact galaxies are old objects experiencing a burst of star formation their position in these diagrams is expected to coincide with that of irregular galaxies, while if they are young objects they are expected to lie below the normal irregulars. The relatively large uncertainties in the observations do not allow us to decide unambiguously between these alternatives; although, as can be seen from these figures, both sets of observations coincide and the old object plus present burst hypothesis is somewhat favored. Additional evidence in this same direction seems to be provided by the M_{tot} vs Z plot where the compact galaxies do not deviate significantly from the relation defined by the irregular galaxies.

A difficulty arises when we consider the M/L ratio of the considered galaxies. As seen from Table 5 the average M_{tot}/L_B^0 ratio is of the order of $3-5 M_{\odot}/L_{B\odot}$ for irregular galaxies and of the order of 1 for blue compact galaxies (this difference is expected since we know from their colors that the latter show at present a fast SFR). Note that Rubin et al. (1978) also find for Sc galaxies an M/L ratio of 2-3. But preliminary results of model calculations as well as the results of Table 2 of Larson and Tinsley (1978) indicate that the calculated M/L_B for such systems is of the order of 0.5 or somewhat less. This discrepancy might be reduced assuming that irregular galaxies are in a quiet period between bursts of star formation and are thus less luminous than average. Alternatively, the adopted masses might have been overestimated. Other explanations are indeed possible. It is clear that this problem should be studied further.

VII. Conclusions

We have presented new observations and derived the chemical composition of irregular and blue compact galaxies; from the chemical compositions and masses of these objects we have found a series of results related to their chemical evolution.

From the new abundance determinations as well as previous data on the Magellanic Clouds we derived a pregalactic helium abundance by mass of $Y_p = 0.228 \pm 0.014$ (3σ) with a further enrichment of the interstellar medium by stellar activity such that $\Delta Y/\Delta Z = 2.8 \pm 0.6$ (1σ).

It is found that the gaseous component of massive galaxies shows a higher heavy element content than less massive galaxies, with a relationship given by: $\log M_{\text{tot}} = (8.5 \pm 0.4) + (190 \pm 60)Z$ where standard deviations of the coefficients are given. This relationship apparently is due to a higher star formation rate for the more massive objects.

By extrapolation of the N/O vs O/H diagram it is estimated that the primary nitrogen to oxygen ratio is given by $\log N(\text{N})/N(\text{O}) < -1.5$ where it is assumed that nitrogen is produced by massive stars. Low mass stars might also be responsible for some primary production. The observed N/O vs O/H diagram shows considerable scatter, we think that a substantial fraction of it is due to observational errors and to a poor knowledge of the electron temperature in the low ionization degree zones. Therefore more observations of higher quality are needed to pursue the problem of secondary and primary nitrogen production.

A linear relation is found between Z and $\ln(M_{\text{gas}}/M_{\text{tot}})$. It is given by

$$Z/10^{-2} = (0.0 \pm 0.2) + (0.4 \pm 0.1) \ln M_{\text{tot}}/M_{\text{gas}}.$$

This result is consistent with the idea that the pregalactic Z value is zero and that under the hypothesis of a simple model of chemical evolution (a closed system with IRA) the slope corresponds to the heavy element yield $p = 0.004 \pm 0.001$, in agreement with other observational determinations. For reasonable IMF's this value of p is consistent only with stellar evolution models with substantial mass loss. The IMF used in this paper is compatible with this yield if we adopt models with large mass loss rate by Chiosi et al. (1978).

We have computed chemical evolution models of closed systems to compare with our observations. We have prepared two sets of models, one with no stellar mass loss and the other with a substantial mass loss. Each set comprises a series of models of different SFR; each model has a constant SFR. In what follows we discuss the main results.

We obtained, as expected, that for those elements produced in stars with $M > 10 M_{\odot}$ IRA is valid. The remaining problem that could affect the value of the yields is the possibility of mass infall or galactic mass loss for the objects under consideration.

We found that $\Delta Y/\Delta Z$ is not very sensitive to variations in the SFR; the values derived for reasonable SFR's are about 40% smaller than those derived under IRA. In addition to the excellent agreement that we obtain between the theoretical and observed heavy element yields for the models with stellar mass loss, these models provide a far better agreement with the observed $\Delta Y/\Delta Z$ ratios than those models without mass loss (see also Chiosi, 1979).

For nitrogen enrichment we have assumed in our models both primary production by massive stars and secondary production by low mass stars. Our models with mass loss imply that only about 10% of carbon in the hydrogen zone is converted into nitrogen. From the very good agreement obtained for p and $\Delta Y/\Delta Z$, this secondary production should be considered as a prediction of the model that can be tested by means of planetary nebulae observations. Alternatively, models without mass loss require a substantial production of nitrogen not only in the hydrogen zone but also in the helium zone.

Our models predict smaller N/O and Y values for a given Z for objects recently formed with a fast SFR than for older objects with a slow SFR and experiencing a burst of star formation. From the observations we do not find a significant trend for the

blue compact galaxies to lie below the irregular galaxies in the N/O–O/H and the Y–Z diagrams. Considering the size of the effect and the quality of the observations the evidence is weak but in favor of the hypothesis that blue compact galaxies are old objects experiencing a burst of star formation. Again, higher quality observations are needed to clarify this point.

The M/L ratios, particularly those for the irregular galaxies, are higher than those predicted by the models. This discrepancy diminishes if the average luminosity of these objects was higher in the past. This problem should be studied further.

References

- Aller, L.H., Czyzak, S.J., Keyes, C.D.: 1977, *Proc. Natl. Acad. Sci.* **74**, 5203
- Alloin, D., Collin-Souffrin, S., Joly, M., Vigroux, L.: 1979, *Astron. Astrophys.* **78**, 200
- Arnett, D.W.: 1978, *Astrophys. J.* **219**, 1008
- Audouze, J., Tinsley, B.M.: 1976, *Ann. Rev. Astron. Astrophys.* **14**, 43
- Balkowski, C., Chamaraux, P., Weliachew, L.: 1978, *Astron. Astrophys.* **69**, 263
- Bergeron, J.: 1976, *Astrophys. J.* **210**, 287
- Bergh, S. van den: 1968, *J. Roy. Astron. Soc. Can.* **62**, 145
- Bertsch, D.L., Fichtel, C.E., Reames, D.V.: 1972, *Astrophys. J.* **171**, 169
- Brocklehurst, M.: 1971, *Monthly Notices Roy. Astron. Soc.* **153**, 471
- Brocklehurst, M.: 1972, *Monthly Notices Roy. Astron. Soc.* **157**, 211
- Butcher, H.: 1977, *Astrophys. J.* **216**, 372
- Chamaraux, P.: 1977, *Astron. Astrophys.* **60**, 67
- Chiosi, C.: 1979, *Astron. Astrophys.* (in press)
- Chiosi, C., Caimmi, R.: 1979, *Astron. Astrophys.* (in press)
- Chiosi, C., Nasi, E., Sreenivasan, S.R.: 1978, *Astron. Astrophys.* **63**, 103
- Crillon, R., Monnet, G.: 1969, *Astron. Astrophys.* **1**, 449
- Cruz-González, C., Recillas-Cruz, E., Costero, R., Peimbert, M., Torres-Peimbert, S.: 1974, *Rev. Mexicana Astron. Astrof.* **1**, 211
- Dufour, R.J.: 1975, *Astrophys. J.* **195**, 315
- Dufour, R.J., Harlow, W.V.: 1977, *Astrophys. J.* **216**, 706
- Dufour, R.J., Killen, R.M.: 1977, *Astrophys. J.* **211**, 68
- Edmunds, M.G., Pagel, B.E.J.: 1978, *Monthly Notices Roy. Astron. Soc.* **185**, 77P
- Faber, S.M.: 1973, *Astrophys. J.* **179**, 731
- Fisher, J.R., Tully, R.B.: 1975, *Astron. Astrophys.* **44**, 151
- Gottesman, S.T., Weliachew, L.: 1972, *Astrophys. Letters* **12**, 63
- Gottesman, S.T., Weliachew, L.: 1977, *Astron. Astrophys.* **61**, 523
- Hayes, D.S., Latham, D.W.: 1975, *Astrophys. J.* **197**, 593
- Houck, N., Cowley, A.P.: 1975, *The University of Michigan Catalogue of two-dimensional Spectral Types for the HD Stars*, Vol. 1, Dept. of Astronomy, University of Michigan, Ann Arbor
- Hindman, J.V.: 1967, *Australian J. Phys.* **20**, 147
- Hubble, E.: 1925, *Astrophys. J.* **62**, 409
- Huchra, J.P.: 1977, *Astrophys. J.* **217**, 928
- Hunt, R.: 1971, *Monthly Notices Roy. Astron. Soc.* **154**, 141
- Iben, I. Jr.: 1977, in 7th Advanced Course of the Swiss Society of Astronomy and Astrophysics
- Iben, I. Jr., Truran, J.W.: 1978, *Astrophys. J.* **220**, 980
- Lambert, D.L.: 1978, *Monthly Notices Roy. Astron. Soc.* **182**, 249
- Lambert, D.L., Luck, R.E.: 1978, *Monthly Notices Roy. Astron. Soc.* **183**, 79
- Larson, R.B., Tinsley, B.M.: 1978, *Astrophys. J.* **219**, 46
- Lequeux, J.: 1979, *Astron. Astrophys.* **71**, 1
- Lequeux, J.: 1979, *Astron. Astrophys.* (in press)
- Lesh, J.R.: 1968, *Astrophys. J. Suppl.* **17**, 371
- Lesh, J.R.: 1972, *Astron. Astrophys. Suppl.* **5**, 129
- Mc Cuskey, S.W.: 1966, *Vistas in Astron.* **7**, 141
- Mc Gee, R.X., Milton, J.A.: 1966, *Australian J. Phys.* **19**, 343
- O'Connell, R.W., Thuan, T.X., Goldstein, S.J.: 1978, *Astrophys. J. Letters* **226**, L11
- Oke, J.B.: 1974, *Astrophys. J. Suppl.* **27**, 21
- Pagel, B.E.J.: 1978, *Monthly Notices Roy. Astron. Soc.* **183**, 1P
- Pagel, B.E.J., Edmunds, M.G., Fosbury, R.A.E., Webster, B.L.: 1978, *Monthly Notices Roy. Astron. Soc.* **184**, 569
- Pagel, B.E.J., Patchett, B.E.: 1975, *Monthly Notices Roy. Astron. Soc.* **172**, 13
- Peimbert, M.: 1975, *Ann. Rev. Astron. Astrophys.* **13**, 113
- Peimbert, M.: 1978a, in *Planetary Nebulae*, IAU Symp. 76, ed. Y. Terzian, Reidel, Dordrecht, p. 215
- Peimbert, M.: 1978b, in *The Large-scale Characteristics of the Galaxy* W.B. Burton (ed.), IAU Symp. 84, Reidel, Dordrecht, (in press)
- Peimbert, M., Rodríguez, L.F., Torres-Peimbert, S.: 1974, *Rev. Mexicana Astron. Astrof.* **1**, 129
- Peimbert, M., Spinrad, H.: 1970a, *Astrophys. J.* **159**, 809
- Peimbert, M., Spinrad, H.: 1970b, *Astron. Astrophys.* **7**, 311
- Peimbert, M., Torres-Peimbert, S.: 1974, *Astrophys. J.* **193**, 327
- Peimbert, M., Torres-Peimbert, S.: 1976, *Astrophys. J.* **203**, 581
- Peimbert, M., Torres-Peimbert, S.: 1977, *Monthly Notices Roy. Astron. Soc.* **179**, 217
- Peimbert, M., Torres-Peimbert, S., Rayo, J.F.: 1978, *Astrophys. J.* **220**, 516
- Pradhan, A.K.: 1978, *Monthly Notices Roy. Astron. Soc.* **183**, 89P
- Rubin, V.C., Ford, W.F. Jr., Thonnard, N.: 1978, *Astrophys. J. Letters* **225**, L107
- Salpeter, E.E.: 1955, *Astrophys. J.* **121**, 161
- Sandage, A., Tammann, G.A.: 1974, *Astrophys. J.* **194**, 559
- Sandage, A., Tammann, G.A.: 1975, *Astrophys. J.* **196**, 313
- Searle, L., Sargent, W.L.W.: 1972, *Astrophys. J.* **173**, 25
- Searle, L., Sargent, W.L.W., Bagnuolo, W.G.: 1973, *Astrophys. J.* **179**, 427
- Seaton, M.J.: 1975, *Monthly Notices Roy. Astron. Soc.* **170**, 475
- Serrano, A.: 1978, Ph. D. Thesis, University of Sussex
- Serrano, A., Peimbert, M.: 1979, (In preparation)
- Shostak, G.S.: 1974, *Astron. Astrophys.* **31**, 97
- Smith, H.E.: 1975, *Astrophys. J.* **199**, 591
- Stone, R.P.S.: 1974, *Astrophys. J.* **193**, 135
- Taff, L.G.: 1974, *Astron. J.* **79**, 1280
- Talbot, R.J. Jr., Arnett, W.D.: 1971, *Astrophys. J.* **170**, 409
- Talbot, R.J. Jr., Arnett, W.D.: 1973, *Astrophys. J.* **186**, 51
- Thuan, T.X., Hart, M.H., Ostriker, J.P.: 1975, *Astrophys. J.* **201**, 756
- Torres-Peimbert, S., Peimbert, M.: 1977, *Rev. Mexicana Astron. Astrof.* **2**, 181
- Vaucouleurs, G. de, Vaucouleurs, A. de, Corwin, H.G. Jr.: 1976, *Second Reference Catalogue of Bright Galaxies*, University of Texas Press, Austin and London
- Vigroux, L., Audouze, J., Lequeux, J.: 1976, *Astron. Astrophys.* **52**, 1
- Weaver, T.A., Zimmerman, G.B., Woosley, S.E.: 1978, *Astrophys. J.* **225**, 1021
- Whitford, A.E.: 1958, *Astron. J.* **63**, 201
- Woerden, H. van, Bosma, A., Mebold, U.: 1975, in *La Dynamique des Galaxies Spirales*, ed. L. Weliachew, Editions du CNRS, Paris, p. 483